

## Parametric Dependence of Turbulent Particle Transport in Tore Supra Plasmas

G. T. Hoang, C. Bourdelle, X. Garbet, J. F. Artaud, V. Basiuk, J. Bucalossi, F. Clairet, C. Fenzi-Bonizec, C. Gil, J. L. Ségui, J. M. Travère, E. Tsitrone, and L. Vermare

*Euratom-CEA Association, CEA/DSM/DRFC, CEA Cadarache F-13108, Saint-Paul-Lez-Durance, France*

(Received 16 April 2004; published 20 September 2004)

Steady state full noninductive current tore supra plasmas offer a unique opportunity to study the local parametric dependence of particle pinch velocity, in order to discriminate among different theories. Magnetic field shear is found to generate an inward pinch which is dominant in the gradient region (normalized radius  $0.3 \leq r/a \leq 0.6$ ). In contrast, the direction of the pinch in the plasma core ( $r/a \leq 0.3$ ) is correlated with the electron temperature gradient length. The results are in agreement with both the turbulent theoretical and computational predictions.

DOI: 10.1103/PhysRevLett.93.135003

PACS numbers: 52.55.Fa, 52.25.Fi, 52.25.Xz

The understanding of the mechanisms responsible for particle transport is of the utmost importance for magnetized fusion plasmas. Indeed, a peaked density profile is attractive to improve the fusion rate which is proportional to the square of the density and to self-generate a large fraction of noninductive current required for continuous operation. Here, from the tore supra results, we will demonstrate the importance of off-diagonal terms in a transport matrix that lead to a peaked density profile.

In some experiments, a neoclassical pinch is high enough to explain the observation of the peaked density profile [1,2]. But in the other cases at DIII-D, JET, TCV [3–5], the existence of an anomalous inward particle pinch has been invoked. Such an anomalous pinch has been unambiguously identified in tore supra [6] thanks to long discharges up to 6 min, totally sustained by a lower hybrid current drive (LHCD) [7] over a time much longer than the current diffusion time (tens of seconds). Under such unique conditions, the electron density profile ( $n_e$ ) remains peaked in steady state. This resilient peaked profile is explained by an inward pinch velocity 2 orders of magnitude above the expected neoclassical value. Such an anomalous pinch can be explained by turbulence theories and simulations [8–10]. The works of Refs. [8,9] invoke two main mechanisms: (i) turbulent thermodiffusion [11,12] generates a pinch velocity, inward or outward, proportional to the inverse of electron gradient length  $\nabla T_e/T_e$ ; (ii) turbulence equipartition (magnetic field curvature) [13,14] drives an inward pinch proportional to the inverse of gradient length of the safety factor  $q$ ,  $\nabla q/q$ . In the present Letter, we demonstrate experimentally that these two types of pinch coexist in tore supra low collisionality plasmas ( $\nu^* = 0.1\text{--}0.35$ ).

In tokamaks, the electron flux is generally described by the following equation:

$$\Gamma = -D[\nabla n_e + (C_q \nabla q/q - C_T \nabla T_e/T_e)n_e] + V_{\text{Ware}} n_e. \quad (1)$$

This formula, including the pinch velocity induced by the

toroidal inductive electric field ( $E_\phi$ ), the Ware pinch ( $V_{\text{Ware}}$ ) [15], clearly shows that it is very difficult to separate different effects when the plasma is inductive because of the complex coupling between  $T_e$ ,  $n_e$ ,  $q$ , and  $E_\phi$  radial profiles through the plasma resistive current. Taking advantage of the very long duration of full non-inductive current tore supra plasmas, the dependences on  $\nabla T_e/T_e$  and on  $\nabla q/q$  have been locally studied in order to discriminate between the two main theoretical predictions mentioned above. These sawtooth-free discharges have been noninductively sustained by the LH waves [7], in the absence of the Ware pinch and with a small central particle source. In these conditions, the density profile peaking is approximately determined from Eq. (1) by

$$\nabla n_e/n_e = -C_q \nabla q/q + C_T \nabla T_e/T_e. \quad (2)$$

The main finding of the present work is that the inward pinch driven by  $\nabla q/q$  is found to be dominant in the gradient region ( $0.3 \leq r/a \leq 0.6$ ). Nevertheless, the direction of the pinch in the plasma core (normalized radius  $r/a \leq 0.3$ ,  $a$  being the plasma minor radius) is rather sensitive to the electron temperature gradient length. These observations are correlated with a change in the type of dominant unstable drift modes in the plasma. In fact, microstability analysis shows that the trapped electron modes (TEM) are dominant in the gradient region, while the ion temperature gradient modes (ITG) dominate in the central part inside  $r/a = 0.3$ .

In tore supra experiments [7], the LHCD deuterium discharges have been realized at plasma current  $I_p = 0.5\text{--}0.7$  MA, toroidal field  $B = 3.8$  T, major radius  $R = 2.4$  m,  $a = 0.71$  m, central density  $n_e(0) = 2\text{--}3.5 \times 10^{19} \text{ m}^{-3}$ , central electron temperature  $T_e(0)$  reaching up to 8 keV, and central ion temperature  $T_i(0) = 1.5\text{--}2$  keV. The loop voltage was kept exactly constant and equal to zero using the real time controls. Thus, after a few tens of seconds, the inductive electric field vanishes throughout the plasma cross section. These plasmas were well diagnosed. Electron density and temperature profiles

are provided by various diagnostics, such as reflectometry, interferometry, Thomson scattering, and a superheterodyne radiometer. In addition, the current density profile was reconstructed by the integrated package of codes CRONOS [16] using the profile of fast electron bremsstrahlung to determine the LHCD current profile. Fast electron profiles are measured by a hard-x-ray tomographic system. The current profile reconstruction is moreover constrained by the polarimetry and plasma self-inductance measurements.

We will first discuss the parametric dependence of the core region  $r/a \leq 0.3$ . When LH power is applied, a flattening of density profile occurs mainly in the plasma core, together with a strong central electron heating [Figs. 1 and 2(b)]. The analysis of current relaxation shows that the change in  $\nabla n_e/n_e$  is correlated to  $V_{\text{Ware}}$  vanishing, rather than to the variation of  $\nabla T_e/T_e$ . Time evolution of different quantities for a 2 min discharge with combining LHCD and ion cyclotron resonance heating (ICRH) is displayed in Fig. 2. Figure 2(b) shows that during the current relaxation (from 6 to 12 s), the local value at  $r/a = 0.3$  of  $\nabla n_e/n_e$  decreases by a factor of about 2 when the Ware pinch drops to zero. While the value of  $\nabla T_e/T_e$  swings between 2 and 4, it is not correlated with the monotonic decrease of  $n_e$  gradient. The neoclassical pinch shown in this figure is computed by NCLASS [17] taking into account all neoclassical effects, including the pinch driven by temperature and the density gradients of all particle species. A weak effect of the thermodiffusion on the density profile can be identified in the plasma core region only when the Ware pinch is completely suppressed. Indeed, as shown in Fig. 2(c), an inward thermodiffusion flux is observed during 20 s, where the neoclassical pinch velocity remains at a constant low level. In this figure, the increase of  $\nabla n_e/n_e$  of about 30% is clearly correlated with increasing  $\nabla T_e/T_e$ .

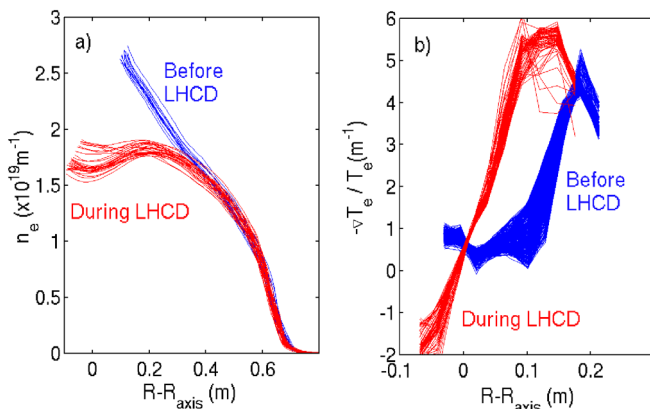


FIG. 1 (color online). (a) Electron density and (b)  $\nabla T_e/T_e$  radial profiles for a 3 min discharge with 3 MW of LH power applied at  $t = 7$  s before (from 4–6 s) and during (from 10–13 s) LHCD.

Weak variations of  $\nabla q/q$  within the error bars cannot explain the change of  $\nabla n_e/n_e$ , as confirmed by the analysis in the next paragraph.

In order to identify clearly the dependence of  $n_e$  upon  $\nabla T_e/T_e$  and  $\nabla q/q$ , a set of seven full LHCD plasmas has been selected. Note that it is necessary to use a set of discharges in order to obtain large variations of  $\nabla T_e/T_e$  and  $\nabla q/q$ , while keeping one of them at a fixed value. For example, because of the stiffness of the  $T_e$  profile [18,19],  $\nabla T_e/T_e$  cannot be changed substantially at a given radial position and at  $\nabla q/q$  constant. The main parameters of this data set are the following:  $n_e(0) = 2.2\text{--}3.5 \times 10^{19} \text{ m}^{-3}$ ,  $q_{\text{edge}} = 9\text{--}14$ ,  $q(0) = 1.2\text{--}2$  without sawteeth,  $T_e(0) = 4.5\text{--}7.8 \text{ keV}$ , and  $T_i(0) = 1.5\text{--}2.5 \text{ keV}$ . For each discharge, the radial profiles are taken over time intervals ranging between 1 and 2 s. We limit our analysis to the region  $r/a \leq 0.6$  in order to avoid the dominant particle source in the outer part of the plasma [6].

$\nabla n_e/n_e$  versus  $\nabla T_e/T_e$  is presented in Fig. 3. Best fits, according to Eq. (2), show two distinguished regions. The direction of the thermodiffusion pinch is found to change when moving from the outer to the inner plasma. The sign of the thermodiffusion pinch is determined by the slope of the curves [coefficient  $C_T$  in Eq. (2)]. The change of the

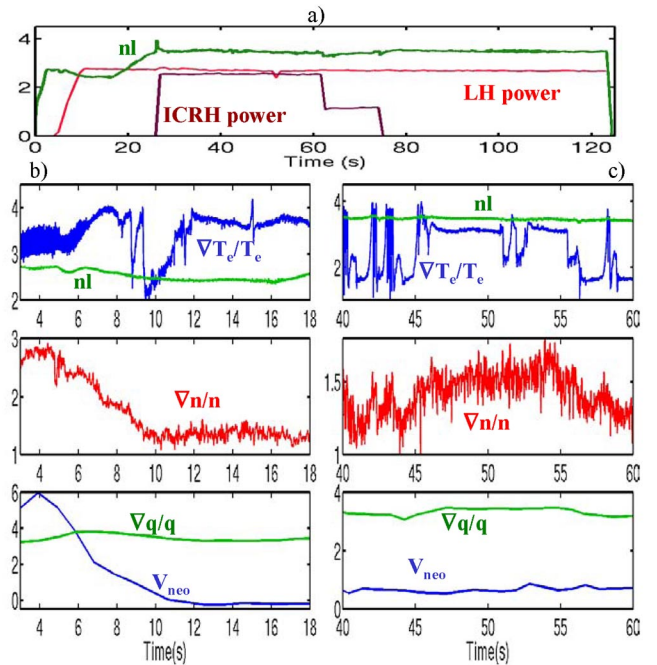


FIG. 2 (color online). Combined ICRH and LHCD discharge: (a) central line density in  $10^{19} \text{ m}^{-2}$ , LH, and ICRH power in MW; (b) correlation between  $\nabla n_e/n_e$  and the Ware pinch at  $r/a = 0.3$ ; (c) correlation between  $\nabla n_e/n_e$  and  $\nabla T_e/T_e$  (in  $\text{m}^{-1}$ ), at  $r/a = 0.3$ , when vanishing Ware pinch ( $V_{\text{neo}}$  in  $10^{-2} \text{ m/s}$ , including all neoclassical effects). Variations of  $\nabla T_e/T_e$  from 40 to 45 s are due to  $T_e$  oscillations described in Ref. [23].

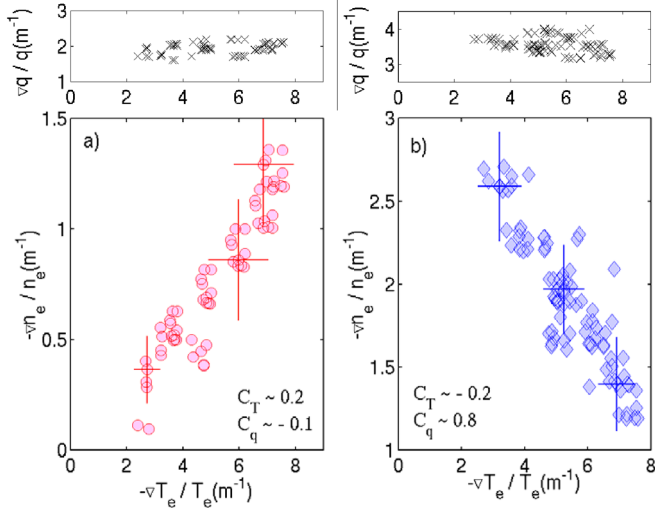


FIG. 3 (color online).  $\nabla n_e/n_e$  versus  $\nabla T_e/T_e$  from a set of seven discharges: (a) for  $r/a \leq 0.30$ ,  $T_e/T_i = 2 \pm 0.4$ ,  $\nabla T_e/\nabla T_i = 3.8\text{--}4.8$ ; (b) for  $0.35 \leq r/a \leq 0.6$ ,  $T_e/T_i = 1.2 \pm 0.4$ ,  $\nabla T_e/\nabla T_i = 0.7\text{--}3.5$ . Corresponding variation of  $\nabla q/q$  is displayed at the top (crosses).

thermodiffusion pinch direction seems to correlate with increasing  $\nabla T_e/\nabla T_i$ , as predicted from the results of Ref. [9]. The ratio  $\nabla T_e/\nabla T_i$  is ranging from 0.7 to 4.8 in the considered case. In the core region  $r/a \leq 0.3$ , an inward thermodiffusion flux is found corresponding to  $C_T > 0$  [Fig. 3(a)]. Figure 3(a) shows an increase of  $\nabla n_e/n_e$  by a factor of about 2.5 when doubling  $\nabla T_e/T_e$ ;  $\nabla q/q$  is kept at the value  $2 \pm 0.4$ ;  $T_e$  is approximately twice  $T_i$ . This is consistent with previous observations in the discharge shown in Fig. 2(c). In addition, the slope and the origin of the linear fit, corresponding, respectively, to  $C_T$  and  $C_q$  in Eq. (2), indicate that the thermodiffusion pinch is stronger than magnetic field curvature pinch. Conversely, in the gradient region  $0.35 \leq r/a \leq 0.6$  [Fig. 3(b)], the thermodiffusion flux is outward and is weaker than the inward curvature flux.

The existence of an inward curvature pinch in the gradient region, within  $0.3 \leq r/a \leq 0.6$ , is also confirmed by analyzing the dependence of the density peaking upon  $\nabla q/q$ , while keeping  $\nabla T_e/T_e$  constant. As shown in Fig. 4, in the gradient region,  $\nabla n_e/n_e$  increases linearly as a function of  $\nabla q/q$  with a positive slope. This figure also shows that the curvature pinch is dominant, since the coefficient  $C_q \approx 0.8$  is higher than  $C_T \approx -0.15$ . This result could explain the correlation between the density profile peaking and the current profile observed in Ref. [20].

Microstability of these discharges has been analyzed with the linear electrostatic gyrokinetic code KINEZERO [21]. The spectra of linear growth rate ( $\gamma$ ) of the unstable electrostatic eigenmodes have been calculated taking into account the nonadiabatic response of both ion and electron populations, covering large ( $k_\theta \rho_i < 1$ , ITG, and

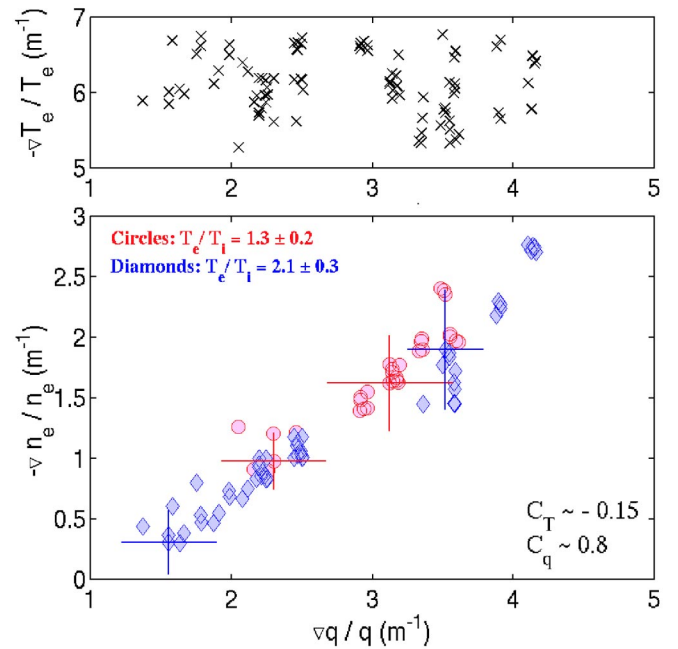


FIG. 4 (color online).  $\nabla n_e/n_e$  versus  $\nabla q/q$  within  $0.3 \leq r/a \leq 0.6$  from a set of seven discharges, keeping  $|\nabla T_e/T_e|$  at the value of  $6 \text{ m}^{-1} \pm 10\%$  (crosses in top) and  $\nabla T_e/\nabla T_i = 0.6 \pm 0.3$ .

TEM) and small scales [ $k_\theta \rho_i > 1$ , TEM, and electron temperature gradient (ETG)] instabilities. In these discharges, the collisionality is relatively low. The electron collision frequency  $\nu_e$  is between  $0.5 \times 10^4 \text{ s}^{-1}$  and  $4 \times 10^4 \text{ s}^{-1}$ , compared to the vertical drift frequency of trapped electrons  $\omega_{De}$  at  $k_\theta r_i = 1$  ranging from  $0.5 \times 10^5$  to  $1 \times 10^5 \text{ s}^{-1}$  for  $r/a = 0.1$  to  $0.6$ , respectively. Thus, the trapped electron contribution is not negligible [22]. The results of the analysis indicate that ITG and TEM are destabilized inside the region  $r/a \leq 0.6$ . While the ETG modes are found to be stable at all radii. TEM are more and more dominant when moving from the core to the gradient zone. Conversely, in the core  $r/a < 0.3$ , the unstable modes are purely ITG. These results are obtained from two calculations. In the first case, the effect of collisions is neglected (i.e.,  $\nu_e/\omega_{De} = 0$ ). In the second case, we neglect the trapped electron contribution (i.e.,  $\nu_e/\omega_{De} \gg 1$ ). The complete spectra of  $\gamma$  calculated at midradius are shown in Fig. 5(a). Radial profiles of maximum growth rate are displayed in Fig. 5(b).

In summary, the parametric dependence studies of anomalous particle pinch observed in tore supra discharges support the turbulent transport theories based on ITG and TEM. Experimentally, we demonstrated that both the thermodiffusion and magnetic field curvature pinches coexist. Ware pinch is found to affect only the central part of the plasma. The electron density profile strongly depends on  $\nabla T_e/T_e$  and  $\nabla q/q$  in full noninductive discharges. In the gradient region ( $r/a = 0.3\text{--}0.6$ ),

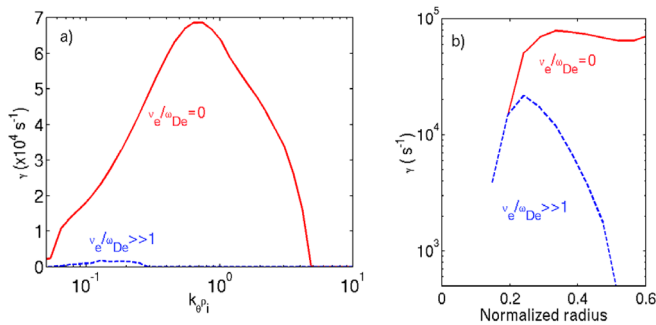


FIG. 5 (color online). Microstability analysis of a full LHCD discharge: (a) spectrum of linear growth rate at miradius; (b) radial profile of maximum growth rate. Solid curves:  $\nu_e/\omega_{De} = 0$ ; dashed curves:  $\nu_e/\omega_{De} \gg 1$  (absence of TEM).

the pinch driven by  $\nabla T_e/T_e$  is outward, but its effect on the density profile is weak. Electron density profile is mainly determined by an inward pinch generated by  $\nabla q/q$  correlated with TEM dominant unstable modes, as predicted by transport simulations [9,10,22]. In contrast, the  $n_e$  profile peaking in the plasma core ( $r/a \leq 0.3$ ) is determined by the temperature gradient driven pinch observed when the Ware pinch is completely suppressed. An inward pinch is observed when increasing  $\nabla T_e/T_e$ , in good correlation with dominant unstable ITG branch. These results also seem to indicate a change of the direction of thermodiffusion flux with the ratio  $\nabla T_e/\nabla T_i$ , as predicted in Ref. [9].

The diligent support of the Tore Supra Team is gratefully acknowledged.

- 
- [1] J. Stober *et al.*, Nucl. Fusion **41**, 1535 (2001).
  - [2] L. Garzotti *et al.*, Nucl. Fusion **43**, 1829 (2003).
  - [3] D. R. Baker *et al.*, Nucl. Fusion **40**, 1003 (2000).
  - [4] M. Valovic *et al.*, Plasma Phys. Controlled Fusion **44**, 1911 (2002).
  - [5] H. Weisen and E. Minardi, Europhys. Lett. **56**, 542 (2001).
  - [6] G. T. Hoang *et al.*, Phys. Rev. Lett. **90**, 155002 (2003).
  - [7] D. Van Houtte *et al.* (to be published).
  - [8] D. R. Baker, Phys. Plasmas **11**, 992 (2004).
  - [9] X. Garbet *et al.*, Phys. Rev. Lett. **91**, 035001 (2003).
  - [10] C. Angioni *et al.*, Phys. Plasmas **10**, 3225 (2003).
  - [11] B. Coppi and C. Spight, Phys. Rev. Lett. **41**, 551 (1978).
  - [12] W. Tang *et al.*, Phys. Fluids **29**, 3715 (1986).
  - [13] M. B. Isichenko, A. V. Gruzinov, and P. H. Diamond, Phys. Rev. Lett. **74**, 4436 (1996).
  - [14] D. R. Baker and M. N. Rosenbluth, Phys. Plasmas **5**, 2936 (1998).
  - [15] A. A. Ware, Phys. Rev. Lett. **25**, 916 (1970).
  - [16] V. Basiuk *et al.*, Nucl. Fusion **43**, 822 (2003).
  - [17] W. A. Houlberg *et al.*, Phys. Plasmas **4**, 3230 (1997).
  - [18] G. T. Hoang *et al.*, Phys. Rev. Lett. **87**, 125001 (2001).
  - [19] F. Ryter *et al.*, Phys. Rev. Lett. **86**, 2325 (2001).
  - [20] H. Weisen *et al.*, Plasma Phys. Controlled Fusion **46**, 751 (2004).
  - [21] C. Bourdelle *et al.*, Nucl. Fusion **42**, 892 (2002).
  - [22] C. Angioni *et al.*, Phys. Rev. Lett. **90**, 205003 (2003).
  - [23] G. Giruzzi *et al.*, Phys. Rev. Lett. **91**, 135001 (2003).